Prediction of Diffraction Effects Due to Irregular Terrain on Radio Wave Propagation in the VHF and UHF Bands

***Emanoel Costa*[1], *Marco Aurélio Nunes da Silva*[1], *and Markus Liniger*[2]**

[1]Centro de Estudos em Telecomunicações, Pontifícia Universidade Católica do Rio de Janeiro (CETUC/PUC-Rio), Rua Marquês de São Vicente 225, 22451-900 Rio de Janeiro RJ BRASIL, e-mails: {epoc,marcoans}@cetuc.puc-rio.br

[2]LiniKomm GmbH, CH-3012 Bern, Switzerland, e-mail: markus_liniger@bluewin.ch

Abstract

Many models have been proposed to represent diffraction effects on the propagation of radio waves over irregular terrain in the VHF and UHF bands. Predictions from these models have been compared with results from associated field-strength measurements available in extensive databases that also incorporate the technical parameters of thousands of VHF and UHF links. Some possible sources of the still high values of the standard deviations of errors between predictions and measurements will be identified and discussed, with particular attention to uncertainties on digital elevation models and on the effective Earth's radius, as well as to effects from lateral propagation.

1. Introduction

Many models are available to predict diffraction effects on the propagation of radio waves over irregular terrain in the VHF and UHF bands that are or will be used by digital TV applications. These effects are generally estimated using: (i) the classical prediction models proposed by Bullington, Epstein-Peterson, and Deygout [1]-[4], with modifications; (ii) the ones described by the most recent versions of Recommendations ITU-R P.526 [5] and ITU-R P.1812 [6], that have been continually improved by work performed over decades and that may be key elements in the path-specific propagation models being developed; (iii) the Longley-Rice model [7].

Another key element in the ongoing modeling effort is the availability of extensive databases assembled the ITU-R Correspondence Group 3K-1 (ITU-R CG3K-1) [8] and the Institute for Telecommunication Sciences (ITS) [9]. These databases incorporate the technical parameters of thousands of VHF and UHF links, including the results from associated field-strength measurements. The predicted field strengths were compared with those from the corresponding measurements. The average values and the standard deviations of the errors between predictions from each of the methods discussed in the previous sections and measured results are displayed in Figure 1, using the number of main obstacles in the terrain profiles as a parameter. The numbers of links in each of these classes can be seen on top of the plots. It is important to initially note that optimistic methods predict field intensities that are greater than the corresponding measured values on average and yield positive values in the left plot of Figure 1. The black curves in both plots indicate results from method that have not applied error-detrending polynomials. These polynomials have only been coupled with the Deygout and the Bullington methods, and the corresponding results are shown by the red curves. It is clearly observed in Figure 1 that the use of detrending polynomial successfully eliminates the average prediction errors and decreases the standard deviations for each of the individual classes of links (characterized by the number of main obstacles) and for the total data set. Some possible sources of the still high values of the standard deviations of errors will be identified and discussed in the next sections.

2. Possible Sources of Errors Between Predictions and Measurements

In addition to instrumental and other errors sources, it should be remembered that the accuracy of digital elevation models is steadily improving but still has limitations and that the field strength measurements described above were not performed in combination with those of the refractivity gradient (or, equivalently, of the effective Earth's radius), in general. One interesting example of such combination of factors can be observed in Figure 2. Most of the above methods do not consider the possibility that strong ground reflections could lead to multipath and cannot predict the observed variations of the field strength with height. At certain heights (for example, 732 m), the prediction error due to the combination of multipath with uncertainties in terrain profile and the effective Earth radius exceeds 20 dB. In the present work, the combined effects of the above sources of errors, represented by random variables, will be quantified through simulations, considering simplified terrain profiles.

978-1-4244-6051-9/11/$26.00 ©2011 IEEE

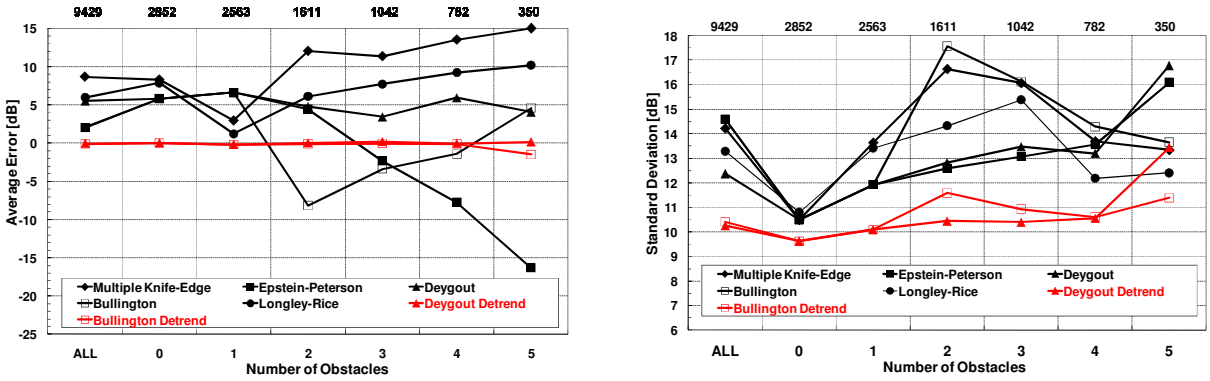

Figure 1. Average (left) and standard deviation (right) values of the errors between calculations and measured results for different prediction methods as functions of the number of main obstacles.

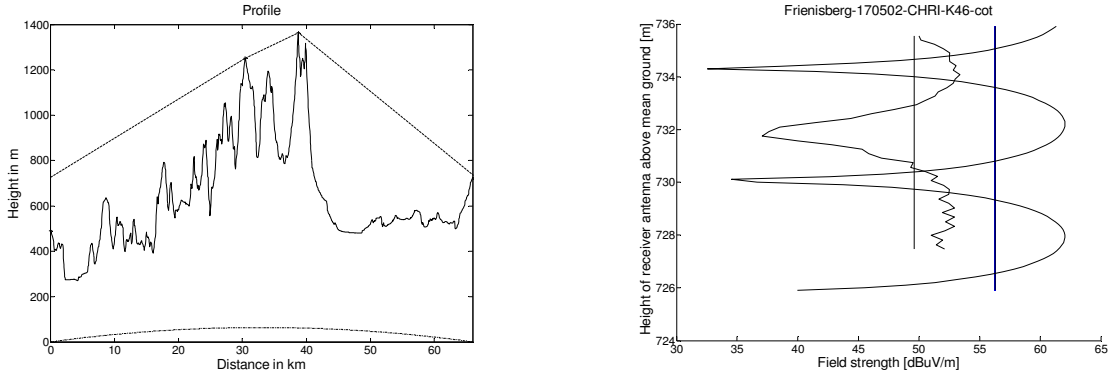

Figure 2. The left plot shows the profile between S. Chrischona (transmitter) and Frienisberg (receiver), with two main obstacles. The right plot shows the calculated (smooth) and measured (irregular) height functions measured at Frienisberg.

It should also be noted that extensive work on the effects of shape of the main terrain obstacles and of ground cover is still in the process of being incorporated into most models.

3. Effects from Lateral Terrain Variations on the Propagation of Radio Waves

All the above are two-dimensional models which neglect propagation outside the vertical plane containing the transmitting and receiving antennas. For some scenarios, this may not be a reasonable assumption. There are relatively few three-dimensional (3D) formulations available in the literature for this problem. The 3D formulation to be described, which could also lead to a better agreement between predictions and measurements, differs from former models in many aspects that will be listed in the next two paragraphs.

The proposed formulation assumes a two-dimensional irregular terrain on top of a smooth spherical Earth. It is developed using spherical coordinates, which naturally and easily accommodates the spreading of the transmitting antenna beam with azimuth. Atmospheric effects are represented by a height-dependent index of refraction. The vector electromagnetic field is expressed in terms of electric and magnetic Hertz potentials, each satisfying a modified scalar Helmholtz equation. This representation automatically guarantees divergent-free electric and magnetic fields at all points of the continuous space. The two Hertz potentials, and consequently also the electromagnetic field components, are coupled by the surface of the irregular terrain through a vector impedance boundary condition. So, depolarization is included in the present formulation. A simple mapping is applied to the region of interest to transform the irregular

terrain into a spherical surface. In the new reference frame, the resulting Helmholtz equation, its parabolic approximation and the components of transformed impedance boundary condition include additional and more complex variable coefficients. On the other hand, the components of the new boundary condition are enforced on a simple spherical surface without approximations. The parabolic equation and the appropriate boundary conditions define an initial value problem that can be solved using a numerical scheme that progresses along the axial direction [10].

This model was used to analyze the field distribution due to a three-dimensional irregular terrain represented in Figure 3, defined by two identical Gaussian obstacles symmetrically located with respect to the central vertical plane containing the transmitter and the receiver. The source produced a vertically-polarized and azimuthally-uniform beam with horizontal axis and Gaussian distribution in elevation characterized by a half-power beamwidth equal to 3°. The transmitter, operating at f = 1 GHz, is located 25 m above the smooth spherical ground with the complex relative permittivity $\varepsilon_r = 80 + i79.1$. Each obstacle is represented by the function

$$h_m(\theta,\varphi) = h_o exp\left\{-\left[\left(\frac{\theta-\theta_{om}}{\Delta\Theta_m}\right)^2 + \left(\frac{\varphi-\varphi_{om}}{\Delta\Phi_m}\right)^2\right]\right\} \quad (1)$$

where m = 1,2; h_o = 50 m; the obstacle centers are located 5 km from the transmitter ($\theta_{om} = 0.04492^o$) and 80 m from each other ($\varphi_{om} = \pm\ 0.45837^o$); $\Delta\Theta_m = 0.00888^o$; and $\Delta\Phi_m = 0.22655^o$. The maximum longitudinal and lateral thicknesses of the isolated obstacles between $h_o/10$ points are 3 km and 60 m, respectively. The maximum height above the smooth spherical ground of the combined terrain profile along the central vertical plane containing the transmitter and the receiver is equal to only 1.67 m at the point (θ_{om}, 0°).

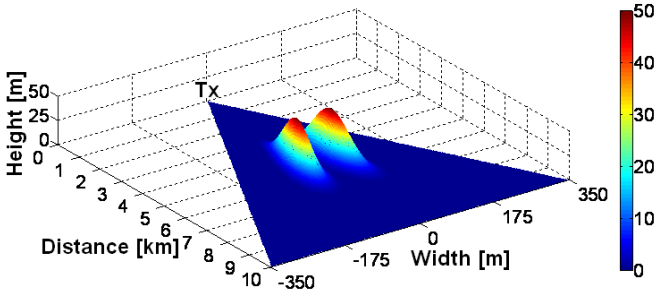

Figure 3. Irregular terrain represented by two Gaussian obstacles on top of a smooth spherical Earth.

Figure 4 shows the height distributions of the propagation factor at 6 km from the source ($\theta = 0.05390^o$) for the azimuth $\varphi = 0°$ according to the proposed (3DP) and a 2D Fourier Split-Step (SST) models. It is observed that: (1) corresponding peak intensities (for example, those above 120 m) may differ by 10 dB; and (2) structures predicted by the proposed 3DP model are not present in the 2D SST results (for example, those between 60 m and 100 m).

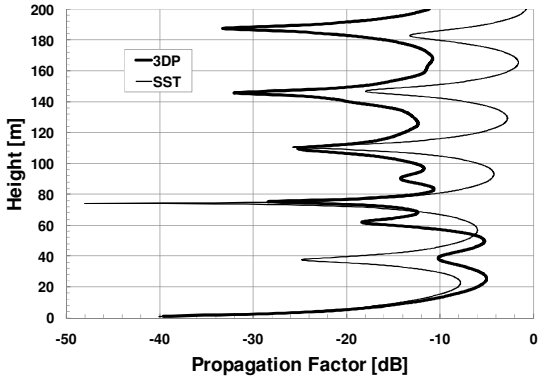

Figure 4. Height distributions of the propagation factor at 6 km from the source for the azimuth $\varphi = 0°$ according to the proposed (3DP) and the 2D Fourier Split-Step (SST) models.

6. Acknowledgments

M. A. N. S. was supported by a grant from Coordenação de Aperfeiçoamento de Pessoal de Nível Superior, Ministério da Educação (CAPES/MEC) during this study.

7. References

1. ITU Handbook, "*Terrestrial Land Mobile Radiowave Propagation in the VHF/UHF Bands,*" International Telecommunication Union, Geneva, Switzerland, 2002.

2. K. Bullington, "Radio Propagation at Frequencies Above 30 Megacycles," *Proc. Inst. Radio Eng.*, **35**(10), October 1947, pp. 1122-1136.

3. J. Epstein and D. W. Peterson, "An Experimental Study of Wave Propagation at 850 Mc/s," *Proc. Inst. Radio Eng.*, **41**(5), May 1953, pp. 595-611.

4. J. Deygout, "Multiple Knife-edge Diffraction of Microwaves," *IEEE Trans. Antennas Propagat.*, **14**(4), July 1966, pp. 480-489.

5. Recommendation ITU-R P.526-11, "Propagation by Diffraction," International Telecommunication Union, Geneva, Switzerland, 2009.

6. Recommendation ITU-R P.1812-1, "A Path-specific Propagation Prediction Method for Point-to-area Terrestrial Services in the VHF and UHF Bands", International Telecommunication Union, Geneva, Switzerland, 2009.

7. G. Hufford, "The ITS Irregular Terrain Model," Institute for Telecommunication Sciences, National Telecommunications and Information Administration, Boulder, CO, U.S.A., 1995.

8. ITU databanks, "SG 3 Databanks: Databanks of VHF/UHF Measurements Relating to Terrestrial Broadcasting," in http://www.itu.int/ITU-R/software/study-groups/rsg3/databanks/vhf-uhf/.

9. http://flattop.its.bldrdoc.gov/propdata/.

10. M. A. N. Silva, E. Costa, and M. Liniger, "Analysis of the Effects from Lateral Variations of Irregular Terrain on Radio Wave Propagation Based on a Three-dimensional Parabolic Equation," *Proceedings of the Fourth European Conference on Antennas and Propagation (EuCAP 2010)*, Barcelona, Spain, 2010, DVD-ROM paper P01P2-1, pp. 1-4.